Integrated intravascular ultrasound and photoacoustic imaging scan head

Bao-Yu Hsieh,[1] Sung-Liang Chen,[2] Tao Ling,[2] L. Jay Guo,[2] and Pai-Chi Li[1,3,*]

[1]*Graduate Institute of Biomedical Electronics and Bioinformatics, National Taiwan University, Taipei, Taiwan*

[2]*Department of Electrical Engineering and Computer Science, University of Michigan, Ann Arbor, Michigan, USA*

[3]*Department of Electrical Engineering, National Taiwan University, Taipei, Taiwan*

**Corresponding author: paichi@cc.ee.ntu.edu.tw*

Received April 19, 2010; revised July 6, 2010; accepted July 20, 2010;
posted August 6, 2010 (Doc. ID 127195); published August 20, 2010

The combination of intravascular ultrasound and intravascular photoacoustic imaging has been proposed for improving the diagnosis of arterial diseases. We describe a novel scan-head design for implementing such multimodality imaging. The proposed device has the potential to achieve a sufficiently small size for clinical intravascular applications. The design aims for efficient image data acquisition for facilitating real-time three-dimensional imaging and reducing the required laser pulse repetition frequency. The integrated scan head consists of a single-element, ring-shaped transducer for sideward ultrasound transmission, a multimode fiber with a cone-shaped mirror for optical illumination, and a single polymer microring with mechanical scanning. The phantom imaging and some experimental results are presented. A microring array can be realized in the future to achieve high-frame-rate intravascular multimodality imaging. © 2010 Optical Society of America

OCIS codes: 170.5120, 110.0110.

Intravascular ultrasound (IVUS) and intravascular photoacoustic (IVPA) imaging are useful for detecting atherosclerotic plaques when attempting to prevent rupture of vulnerable plaques. Vulnerable plaques with thin fibrous caps and lipid-rich cores have a high rupture risk in the coronary arteries, and they may also block the blood supply to the heart, resulting in acute myocardial infarction with a high mortality rate [1–4]. These plaques can be distinguished using IVPA imaging based on lipid accumulation exhibiting certain characteristics of optical absorption. The anatomical details of vessels and plaques can be obtained using IVUS imaging [5].

Obtaining high-resolution IVUS images requires high-frequency ultrasound at above 20 MHz, whereas photoacoustic signals from soft tissue have main frequency components below 10 MHz [6]. A wideband acoustic receiving device is necessary for integrated IVUS/IVPA imaging. Furthermore, the size of the transducer is limited by the diameter of the arteries, which are mainly of the order of millimeters. Unfortunately, typical piezoelectric transducers have a relatively narrow bandwidth. Moreover, complicated back-end circuitry is required for array transducers.

To alleviate the above problems, a polymer microring resonator is proposed for acoustic detection in this study. The microring device consists of an input/output bus waveguide and a coupled polystyrene ring waveguide that serves as an optical cavity. The incoming acoustic wave deforms the ring waveguide, which induces a corresponding change in the effective refractive index, resulting in a shift of the resonant wavelength. The acoustic waveform can be recovered by detecting the optical output intensity of the bus waveguide [7]. The microring device has several advantages, including small size (10–100 μm), wide bandwidth (from dc to over 90 MHz at –3 dB), adequate signal-to-noise ratio (SNR) (noise-equivalent pressure $= 0.23$ kPa over 1–75 MHz), ease of fabrication, and no requirement for complicated back-end circuitry [8], which makes it a good candidate for IVUS/IVPA multimodality imaging. Moreover, the level of the noise received by the microring does not vary with the detector size. This unique characteristic can be utilized to meet the size requirement of IVUS/IVPA without compromising the SNR. In contrast to a conventional piezoelectric transducer, the microring is easy to fabricate by nanoimprinting techniques. A single bus waveguide can be used for the microring array [9], thus avoiding complicated back-end circuitry. Therefore, the potential usefulness of the polymer microring resonator in intravascular imaging applications is tested in this study.

Real-time IVUS/IVPA imaging is desirable in clinical applications. The use of a high imaging frame rate can avoid motion artifacts and shorten the data acquisition time, thus lowering the risk of blood clot formation. The pulse repetition frequency (PRF) of a high-power solid-state pulse laser is limited to a few tens of hertz, which makes real-time imaging difficult if a laser pulse is needed for each scan line. We propose a method for high-frame-rate intravascular imaging that employs 360° wave excitation and a microring array surrounding the catheter. This design means that the acoustic waves are detected in parallel, so the frame rates are identical to the PRF of the laser. This technique can be applied to achieve fast three-dimensional (3D) IVUS/IVPA imaging by moving the catheter along the vessel axis.

The scan head was designed as shown in Fig. 1. It consists of a ring-shaped piezoelectric transducer for 360° ultrasound transmission and an illuminating device constructed from a multimode fiber with a cone-shaped mirror for 360° optical illumination. A polymer microring resonator array can be potentially incorporated in the future for acoustic detection. For demonstration purposes, a single microring resonator is used in this study.

The homemade ring transducer is a single-element, side-looking, ring-shaped ultrasonic transducer made of 10° rotated, Y-cut lithium niobate ($LiNbO_3$, LN) that is used for ultrasonic transmission. Figure 2 shows the fabrication procedures of the ring transducer. First, a

 © 2010 Optical Society of America

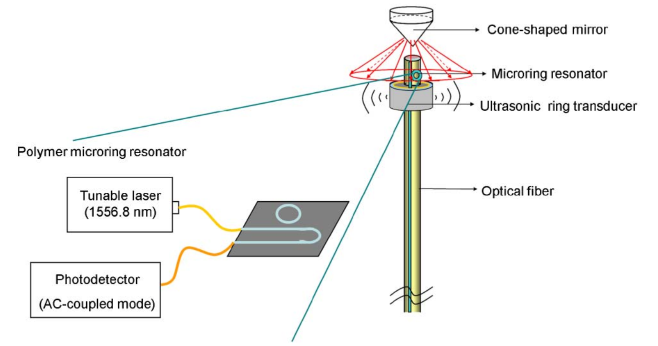

Fig. 1. (Color online) Configuration of the integrated IVUS/IVPA imaging probe consisting of the ring transducer, the illuminating device, and the microring resonator.

doughnut-shaped LN shell with a thickness of 300 μm was created using an ultrasonic sculpturing machine. The inside and outside of the LN shell used as the electrode were coated with chrome and gold (Cr/Au) layers using a sputtering machine. The hole of the LN shell was filled with a high-attenuation material (electrically conductive adhesive) as the backing layer to reduce acoustic ringdown. Silver epoxy was then coated on the negative electrode using a spin coater as the first matching layer, and a 1 mm diameter hole was drilled in the center of the transducer for placing the illuminating optical fiber. A BNC connector was connected to the ring transducer. Finally, Parylene C was coated as the second matching layer onto the surface of the transducer. The performance of the constructed transducer was tested using pulse-echo measurements from a metal plate. The waveform received by the ring transducer and the corresponding spectrum are shown in Fig. 3. The ring-shaped piezoelectric transducer had a center frequency of 16 MHz and a −6 dB bandwidth of 15%. The bandwidth is small because the thickness of the backing layer is limited by the size of the transducer—the thickness was about 0.5 mm, so it does not provide sufficient attenuation.

A tunable Ti:sapphire pulsed laser (CF-125, SOLAR TII, Minsk, Belarus) with a 10 Hz PRF (pulse duration = 15–20 ns) was used for optical illumination. The laser light was coupled into a high-NA (NA = 0.22) multimode optical fiber (Thorlabs, Newton, New Jersey) with a focusing lens. The microcone mirror (Edmund Optics, Barrington, New Jersey) with a diameter of 2 mm was positioned at the terminal end of the fiber tip to increase the sideward-propagating energy of the light (to about 1 mJ) and provide 360° optical illumination without requiring the optical fiber to be rotated.

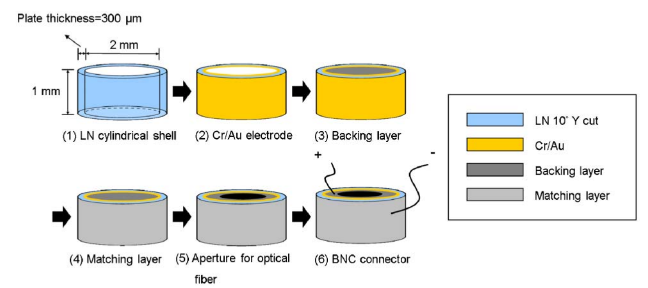

Fig. 2. (Color online) Fabrication procedures and schematic view of the piezoelectric ring transducer.

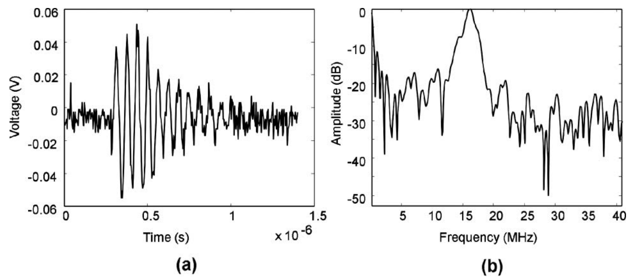

Fig. 3. (a) Pulse-echo signal from the metal plate received by the ring transducer, and (b) spectrum of the pulse-echo signal.

The polymer microring resonator used in this study consisted of a 100 μm diameter polystyrene ring waveguide coupled to an input/output bus waveguide. To position the microring device at the tip of the integrated transducer, a new arrangement with the ring waveguide coupled to a bent-back bus waveguide was designed to be the input and output fiber on the same side of the device, which makes it suitable for IVUS/IVPA clinical use, as shown in Fig. 1. The input fiber was connected to a cw tunable laser (HP 8168F, Agilent Technologies, Santa Clara, California), and the output fiber was connected to a high-speed photodetector (1811-FC, New Focus, San Jose, California) with a gain of 4×10^4 V/A and an electrical bandwidth of dc to 125 MHz.

In photoacoustic imaging, the laser light is reflected from a microcone mirror to shine on the entire cross section of the target to induce a photoacoustic signal, with the generated photoacoustic signal being detected by a microring resonator. Moreover, the same microring resonator can detect the echo signal of the ultrasound transmitted by the ring transducer, which was connected to the pulser/receiver (5077PR, Panametrics Inc.). The photoacoustic and ultrasound images both can be obtained from the integrated catheter. A single-element microring resonator was used to demonstrate the method in the present study. We used this integrated probe to acquire the ultrasound and photoacoustic images of a black plastic tube by rotating the sample, as shown in Fig. 4. The images were processed through the following steps. The detected acoustic signals were digitized at 200 Msamples/s (CS14200, GaGe Applied Inc.). Signal averaging (16 for photoacoustic and 32 for ultrasound) was applied to improve the SNR. There were 240 A-lines recorded per image. Then, the photoacoustic signals were filtered (1–10 MHz) and Hilbert transform was applied for envelope detection. Finally, both the IVPA and IVUS images were scan converted

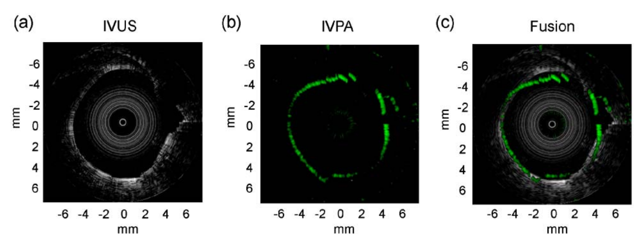

Fig. 4. (Color online) (a) Ultrasound image, (b) photoacoustic image, and (c) fusion image of the black plastic tube acquired by the integrated IVUS/IVPA imaging probe.

from the polar coordinate to the Cartesian system. A fusion image of both modalities is formed. The signal processing steps are similar to what we found in the literature [5]. The –3 dB axial resolution was measured at 0.19 mm/0.28 mm for photoacoustic/ultrasound imaging, respectively.

In this study, we successfully fabricated a ring transducer for 360° ultrasound transmission and demonstrated the feasibility of the integrated IVUS/IVPA scan head using phantom imaging results. The integrated IVUS/IVPA imaging probe we fabricated had a diameter of 3 mm, which is still larger than clinically used imaging catheters. Although the overall diameter of our current fully assembled IVUS/IVPA imaging catheter was 0.5 mm larger than that in [10], our design with 360° excitation has potential to implement ultra-high-frame-rate imaging. Moreover, the probe could be miniaturized by using a small-diameter optical fiber and fabricating a small-element ring transducer.

In our device, a multimode optical fiber coupled to a microcone mirror illuminates the sample with optical energy, and a polymer microring resonator with a wide detection bandwidth detects high-frequency ultrasound for IVUS imaging and low-frequency photoacoustic signals for IVPA imaging. This scan head design has the potential to achieve ultra-high-frame-rate 2D and real-time/near-real-time 3D intravascular imaging, which can be very helpful in clinical diagnosis.

Support from the National Science Council of Taiwan (NSCT) and the National Taiwan University Center for Advanced Nano-Materials is greatly appreciated.

References

1. M. Naghavi, P. Libby, E. Falk, S. W. Casscells, S. Litovsky, J. Rumberger, J. J. Badimon, C. Stefanadis, P. Moreno, G. Pasterkamp, Z. Fayad, P. H. Stone, S. Waxman, P. Raggi, M. Madjid, A. Zarrabi, A. Burke, C. Yuan, P. J. Fitzgerald, D. S. Siscovick, C. L. de Korte, M. Aikawa, K. E. J. Airaksinen, G. Assmann, C. R. Becker, J. H. Chesebro, A. Farb, Z. S. Galis, C. Jackson, I. K. Jang, W. Koenig, R. A. Lodder, K. March, J. Demirovic, M. Navab, S. G. Priori, M. D. Rekhter, R. Bahr, S. M. Grundy, R. Mehran, A. Colombo, E. Boerwinkle, C. Ballantyne, W. Insull, Jr., R. S. Schwartz, R. Vogel, P. W. Serruys, G. K. Hansson, D. P. Faxon, S. Kaul, H. Drexler, P. Greenland, J. E. Muller, R. Virmani, P. M. Ridker, D. P. Zipes, P. K. Shah, and J. T. Willerson, Circulation **108**, 1772 (2003).
2. L. H. Arroyo and R. T. Lee, Cardiovasc. Res. **41**, 369 (1999).
3. E. Falk, P. K. Shah, and V. Fuster, Circulation **92**, 657 (1995).
4. R. T. Lee and P. Libby, Arterioscler. Thromb. Vasc. Biol. **17**, 1859 (1997).
5. S. Sethuraman, S. R. Aglyamov, J. H. Amirian, R. W. Smalling, and S. Y. Emelianov, IEEE Trans. Ultrason. Ferroelectr. Freq. Control **54**, 978 (2007).
6. P. C. Li, C. W. Wei, and Y. L. Sheu, Opt. Express **16**, 20215 (2008).
7. S. Ashkenazi, C. Y. Chou, L. J. Guo, and M. O'Donnell, Appl. Phys. Lett. **85**, 5418 (2004).
8. S. W. Huang, S. L. Chen, T. Ling, A. Maxwell, M. O'Donnell, L. J. Guo, and S. Ashkenazi, Appl. Phys. Lett. **92**, 193509 (2008).
9. C. Y. Chao, S. Ashkenazi, S. W. Huang, M. O'Donnell, and L. J. Guo, IEEE Trans. Ultrason. Ferroelectr. Freq. Control **54**, 957 (2007).
10. A. B. Karpiouk, B. Wang, and S. Y. Emelianov, Proc. SPIE **7564**, 756408 (2010).